ACS Chemical Neuroscience

Article

A Novel F-Labeled Radioligand for Positron Emission Tomography Imaging of 11#-Hydroxysteroid Dehydrogenase (11#-HSD1): Synthesis and Preliminary Evaluation in Nonhuman Primates

Evan Baum, Wenjie Zhang, Songye Li, Zhengxin Cai, Daniel Holden, and Yiyun Huang

ACS Chem. Neurosci., **Just Accepted Manuscript** • DOI: 10.1021/acschemneuro.8b00715 • Publication Date (Web): 28 Jan 2019

A Novel ^{18}F-Labeled Radioligand for Positron Emission Tomography Imaging of 11β-Hydroxysteroid Dehydrogenase (11β-HSD1): Synthesis and Preliminary Evaluation in Nonhuman Primates

Evan Baum[1§], Wenjie Zhang[2§], Songye Li[1]*, Zhengxin Cai[1]*, Daniel Holden[1], Yiyun Huang[1]

[1]PET Center, Department of Radiology and Biomedical Imaging, Yale University School of Medicine, 801 Howard Ave, New Haven, CT 06520-8048

[2]Department of Nuclear Medicine, West China Hospital, Sichuan University, Chengdu, Sichuan 610041, China

[§]These two authors contribute equally to this work

*Corresponding authors

Content graphic

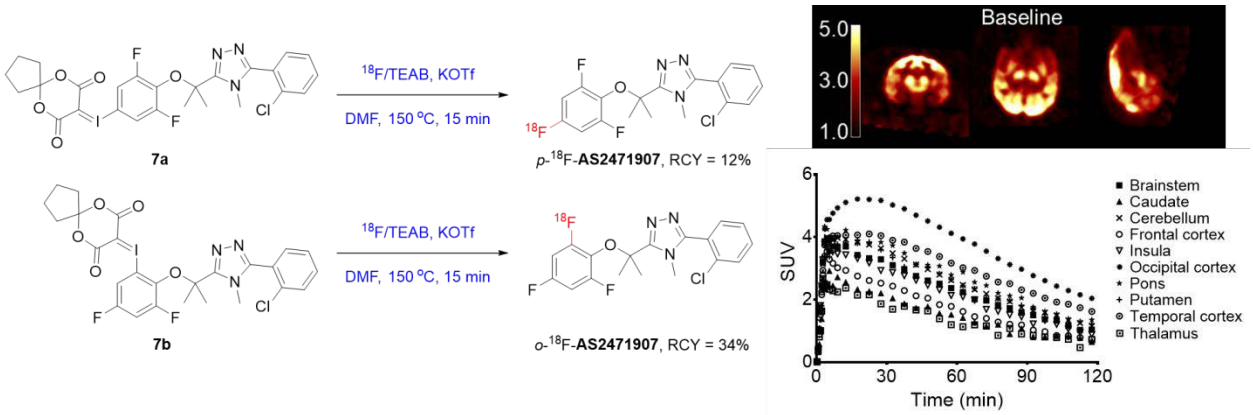

ABSTRACT

11β-hydroxysteroid dehydrogenase type 1 (11β-HSD1) catalyzes the conversion of cortisone to cortisol and controls a key pathway in the regulation of stress. Studies have implicated 11β-HSD1 in metabolic diseases including type 2 diabetes and obesity, as well as stress-related disorders and neurodegenerative diseases, such as depression and Alzheimer's disease (AD). We have previously developed [^{11}C]AS2471907 as a PET radiotracer to image 11β-HSD1 in the brain of nonhuman primates and humans. However, the radiosynthesis of [^{11}C]AS2471907 was unreliable and low-yielding. Here, we report the development of the ^{18}F-labeled version [^{18}F]AS2471907, including the synthesis of two iodonium ylide precursors and the optimization of ^{18}F-radiosynthesis. Preliminary PET experiments, composed of a baseline scan of [^{18}F]AS2471907 and a blocking scan with the reversible 11β-HSD1 inhibitor ASP3662 (0.3 mg/kg), was also conducted in a rhesus monkey to verify the pharmacokinetics of [^{18}F]AS2471907 and its specific binding in the brain. The iodonium ylide precursors were prepared in a 7-step synthetic route with an optimized overall yield of ~2%. [^{18}F]AS2471907 was synthesized in good radiochemical purity, with the *ortho* regioisomer of iodonium ylide providing greater radiochemical yield as compared to the *para* regioisomer. In monkey brain, [^{18}F]AS2471907 displayed high uptake and heterogenous distribution, while administration of the 11β-HSD1 inhibitor ASP3662 significantly reduced uptake, thus demonstrating the binding specificity of [^{18}F]AS2471907. Given the longer half-life of F-18 and feasibility for central production and distribution, [^{18}F]AS2471907 holds great promise to be a valuable PET radiotracer to image 11β-HSD1 in the brain.

Keywords:

11β-HSD1, 11-beta hydroxysteroid dehydrogenase type 1, positron emission tomography, AS2471907, nonhuman primates, radiofluorination.

INTRODUCTION

The 11β-hydroxysteroid dehydrogenases (11β-HSD) catalyze the interconversion of active glucocorticoids to inactive 11-keto forms, thus regulating glucocorticoid access to steroid receptors. In humans, two isozymes, 11β-hydroxysteroid dehydrogenase type 1 (11β-HSD1) and type 2 (11β-HSD2), interconvert cortisone and cortisol through NADPH- and NAD^+-dependent reactions, respectively (Fig. 1).[1] 11β-HSD2 is found primarily in tissues targeted by aldosterone, such as kidney, colon, salivary, and sweat glands. Genetic deficiencies of 11β-HSD2 lead to an excess of cortisol, which cross-reacts with non-selective mineralcorticoid receptors in the distal nephron and causes hypertension, hypokalemia, and other symptoms of apparent mineralcorticoid excess.[1, 2] 11β-HSD1 is widely distributed in metabolically active organs such as the liver, adipose tissue, skeletal muscle, and central nervous system (CNS), where it has high yet uneven expression in the cerebellum, hippocampus, and cortex regions.[1, 3] 11β-HSD1 overexpression in adipose tissue of transgenic mice leads to obesity, insulin resistance, hyperlipidemia, and hypertension, while targeted overexpression in the liver leads to these same symptoms of metabolic syndrome without associated obesity.[4-6] Compared to non-diabetic patients, obese diabetic patients have been found to have elevated or sustained levels of 11β-HSD1 in the liver, implicating the enzyme as a potential target for treatment of type 2 diabetes mellitus and concurrent cardiovascular conditions.[3, 7] In the CNS, 11β-HSD1 deletion or inhibition has been shown to mitigate the age-associated cognitive decline in mice,[8, 9] while administration of the 11β-HSD1 inhibitor UE-2316 was found to improve cognitive function in a mouse model of Alzheimer's disease (AD) independent of Aβ plaque formation.[10] Sandeep *et al.*[11] reported that in both healthy elderly men and type 2 diabetic patients, treatment with the 11β-HSD1 inhibitor carbenoxolone improved verbal fluency and memory, further implicating that local reduction of glucocorticoids in the brain improves cognition.

Due to its association with diabetes, metabolic syndrome, age-related cognitive decline, and AD, 11β-HSD1 has thus become an attractive target for investigation of disease mechanisms and therapeutic development. A Positron Emission Tomography (PET) radiotracer targeting the 11β-HSD1 would allow for noninvasive imaging of the enzyme *in vivo* to better understand its expression under normal and pathological states. PET imaging is also invaluable in evaluating the target occupancy and efficacy of novel 11β-HSD1 inhibitors in many clinical trials, such as ABT-384,[12, 13] UE-2343,[14] PF-915275,[15] MK0916,[16] BMS-770767[17] and ASP3662[18] (Fig. 2).

Molecules targeting 11β-HSD1 employ several structural motifs, including triazole, amide, and sulfonamide groups (Fig. 2). A highly specific triazole compound 3-(2-chlorophenyl)-4-methyl-5-(2-(2,4,6-trifluorophenoxy)propan-2-yl)-4H-1,2,4-triazole (**8**, AS2471907, Fig. 2) was recently reported[19] , which displayed an IC_{50} of 5.6 nM for human 11β-HSD1, >10,000 nM for human 11β-HSD2, and no affinities or cross-activities for various receptors, ion channels, transporters and other enzymes. The ^{11}C-labeled form, [^{11}C]AS2471907 ([^{11}C]**8**), was shown to be a promising radiotracer for imaging brain 11β-HSD1 in monkeys[20] and humans.[21] However, the radiosynthesis of [^{11}C]AS2471907 was unreliable and low-yielding, as it produced three regioisomers with the desired radiotracer as the minor product (Scheme 1). Besides, ^{11}C-labeled radiotracers, in general, have limitations in their applications due to the short radioactive half-life ($t_{1/2}$ = 20.4 min) of the radionuclide and thus the requirement of an onsite cyclotron for their production. The three aromatic fluorine atoms in AS2471907 (**8**) present the opportunity for ^{18}F-labeling. While aromatic rings without strongly electron-withdrawing substituents are difficult to radiofluorinate,[22, 23] recent developments in radiofluorination methodologies provided additional avenues for radiofluorination. For example, using the recently developed iodonium ylides as precursor for ^{18}F-fluorination,[24, 25] we have successfully prepared the κ-opioid receptor antagonist

radiotracer [^{18}F]LY2459989,[26] which could not be accessed through conventional radiofluorination method. We have since translated this chemistry to the preparation of ^{18}F-labeled AS2471907 ([^{18}F]**8**).

In this report we detail the chemical synthesis of two novel iodonium ylide precursors 8-((4-((2-(5-(2-chlorophenyl)-4-methyl-4H-1,2,4-triazol-3-yl)propan-2-yl)oxy)-3,5-difluorophenyl)-λ^3-iodaneylidene)-6,10-dioxaspiro[4.5]decane-7,9-dione (**7a**, Scheme 1) and 8-((2-((2-(5-(2-chlorophenyl)-4-methyl-4H-1,2,4-triazol-3-yl)propan-2-yl)oxy)-3,5-difluorophenyl)-λ^3-iodaneylidene)-6,10-dioxaspiro[4.5]decane-7,9-dione (**7b**, Scheme 1), and discuss the optimization of the radiofluorination with the *para*-regioisomer **7a** to produce *p*-[^{18}F]**8**, which was further refined with the *ortho*-regioisomer **7b** to provide the most efficient radiolabeling with the highest molar activity in the production of [^{18}F]**8**. A preliminary *in vivo* evaluation of this first ^{18}F-labeled 11β-HSD1 PET radiotracer [^{18}F]**8** in non-human primates is also described.

RESULTS AND DISCUSSION

Precursor synthesis

Based on the recent use of iodonium ylide precursors for ^{18}F-labeling,[26-28] a synthetic strategy was devised to produce both the *para*- and *ortho*- iodonium ylide precursors **7a** and **7b** with the 6,10-dioxaspiro[4.5]decane-7,9-dione (**9**, SPI-5) spirocyclic auxiliary attached to the aromatic iodine (Scheme 2). 2,6-difluorophenol (**1a**) and 2,4-difluorophenol (**1b**) were first iodinated, followed by a substitution reaction with ethyl 2-bromoisobutyrate to produce the ester intermediates **2a** and **2b**. Hydrolysis, then coupling with 2-chlorobenzohydrazide yielded **4a** and **4b**, which were cyclized with 2-chloro-1,3-dimethylimidazolinium chloride (DMC) to afford the oxidiazoles **5a** and **5b**. Conversion of **5a** and **5b** to the corresponding triazoles **6a** and **6b** proved

to be the most challenging step, requiring fresh trifluoroacetic acid (TFA) for the in house preparation of methylamine trifluoroacetate ($MeNH_2$-TFA), followed by heating at 150 ^oC for 48 h over molecular sieves. The synthesis of SPI-5 (**9**) was achieved through the reaction of malonic acid and cyclopentanone in the presence of acetic anhydride and concentrated sulfuric acid, as described previously.[26] The aromatic iodine in **6a** and **6b** was oxidized with oxone and TFA, followed by addition of **9** under basic conditions to form the *para*- and *ortho*-iodonium ylides (**7a** and **7b)** as radiolabeling precursors. Both **7a** and **7b** were fully characterized by melting point, ^1H and ^{13}C NMR, and HRMS, with purity of > 98% based on HPLC analysis. The overall yield for the synthetic pathway in Scheme 1 was ~2.2%.

Radiochemistry

Radiolabeling test-run and optimization were first performed using the *para*-iodonium ylide precursor **7a**. Mossine *et al.*[29] detailed the Cu-mediated ^{18}F-fluorination of boronic acids using potassium trifluoromethanesulfonate (KOTf) and potassium carbonate (K_2CO_3) to elute the ^{18}Ffluoride from the ion exchange cartridge, followed by drying and aliquoting small amounts of the resulting base and [^{18}F]KF mixture to perform radiolabeling tests. They described the optimal conditions as having 0.09 μmol of KOTf and 0.012 μmol of K_2CO_3 with 4.0 μmol of precursor in 0.10 mL of solvent. These low base aliquot conditions were assessed with 2.0-2.5 mg of precursor **7a** to screen the solvents for radiolabeling, as shown in Table 1, entry 1-3. Acetonitrile (MeCN), *N,N*-dimethylformamide (DMF), and dimethyl sulfoxide (DMSO) were tested at various temperatures, with the radiochemical conversion (RCC) of **7a** to *p*-[^{18}F]**8** determined by analytical HPLC. The radiolabeling proceeded with maximal conversion of 8% at 200 ^oC in DMF, while no product was formed when MeCN or DMSO was used as solvent. These results were in agreement

with past reports, which found DMF to be the preferred solvent for radiofluorination of a variety of iodonium ylide substrates,[24] as well as diaryliodonium salts.[30, 31] All subsequent reactions were thus performed in DMF.

The method of aliquoting small amounts of dried [^{18}F]KF to achieve low concentrations of base, however, is not practical for routine production of a PET radiotracer, where larger amount of the radioactive product is desired for imaging studies. Furthermore, eluting with such low concentrations of base may result in poor elution efficiency,[29] or necessitate backwashing of ^{18}Ffluoride trapping cartridge,[32] which cannot be easily translated to an automated synthesis module. For these reasons, a series of bases and additives in different amounts were tested in reactions at different temperatures (Table 1, entry 4-13). Addition of Kryptofix 222 or 18-crown-6 with KOTf and K_2CO_3 resulted in low conversion to product. RCC increased to a maximum of 12.4% with 5.0 mg (26.5 μmol, 6.6 eq.) of KOTf and increasing amounts of tetraethylammonium bicarbonate (TEAB) up to 2.0 mg (10.5 μmol, 2.6 eq.), which also provided good (> 90%) elution efficiency. These optimized conditions (Table 1, entry 12) for precursor **7a** were translated to a GE TRACERlab FXN Pro automated synthesis module. Radiolabeling, purification, and formulation of **7a** produced *p*-[^{18}F]**8** with > 99% radiochemical purity by analytical HPLC. Average product activities after formulation were sufficient for monkey imaging studies (0.41 ± 0.31 GBq, n = 11), while molar activities (A_m) at end of synthesis (EOS) were moderate (28.5 ± 9.9 GBq/μmol, n = 11). The radiochemical yield (RCY), calculated as isolated product activity/trapped activity, was low, with an average of 0.5%. The total synthesis time was 88 ± 4 min (n = 11).

The optimized conditions for *para*-iodonium ylide precursor **7a** were tested and further refined on the *ortho*-iodonium ylide precursor **7b**, leading to improved RCC and RCY. The KOTf

and TEAB condition was tried alongside with other bases in DMF at 150 or 160 °C (Table 2). RCC increased to 22% with **7b** (entry 1, Table 2) when heating at 150 °C for 20 min with KOTf (5 mg) and TEAB (2 mg), as compared to 12.4% with **7a** under the same conditions. Use of tetrabutylammonium trifluoromethanesulfonate (TBAOTf) with or without cesium carbonate (Cs_2CO_3) resulted in low RCC. Meanwhile, addition of 2 mg TEAB alone provided an RCC of 34%, and increasing amounts of TEAB up to 16 mg did not increase the conversion rate. The use of 2-10 mg of TEAB in 0.2-0.5 mL of DMF has been shown to be ideal for radiofluorination of iodonium ylides in past studies[24, 26] as well, while greater amounts of base may lead to decomposition of the precursors, therefore decrease RCC. The optimal condition for **7b** (Table 2, entry 4) was adopted to the FXN Pro module to produce *o*-[^{18}F]**8** for PET scans in nonhuman primates. Use of the *ortho*-precursor **7b** afforded *o*-[^{18}F]**8** in > 99% radiochemical purity by analytical HPLC. Average isolated product activity after formulation were 1.02 ± 0.68 GBq (n = 18) with greatly improved EOS A_m of 121.5 ± 101.4 GBq/μmol (n = 18), four times higher than that of radiofluorination with **7a**. RCY increased by six-fold at 3.2 ± 2.1% (n = 18). Total synthesis time on the FXN Pro module was 84 ± 5 min (n = 14). Based on higher RCC, RCY, and A_m, the automated, optimized synthesis using the *ortho*-precursor **7b** will be used for subsequent studies of [^{18}F]**8** in nonhuman primates and translation to clinical studies in human.

Rotstein *et al.*[25] have proposed a mechanism for the radiofluorination of spirocyclic iodonium ylides that involves regioselective reductive elimination. More sterically hindered compounds such as **7a** and **7b** are typically poor substrates for reductive elimination. Reductive elimination of unsymmetrical diaryliodonium salts, however, demonstrates a preference for *ortho*-substituted arenes, including those with an *ortho* methoxy group.[33] A similar *ortho* preference was observed in the radiolabeling of *ortho- vs. para*-benzyloxyphenyliodonium ylides.[25] Furthermore,

computer modeling of *ortho- vs. para*-methoxyphenyliodonium ylides shows a 5 kcal/mol lower $\Delta G^{\ddagger}$ for the *ortho* reductive elimination transition state, indicating that iodonium ylides *ortho* to an alkoxy moiety may undergo radiofluorination with lower activation energies.[25] With less steric destabilization, *para*-iodonium ylides adopt a planar configuration that requires additional energy to rotate the arene to an out-of-plane transition state for reductive elimination.[25] These mechanistic considerations support the observations in this study, that the *ortho*-iodonium ylide **7b** demonstrated more efficient radiolabeling than the *para* compound **7a**, perhaps due to a lower energy barrier to the transition state.

PET Imaging in Nonhuman Primates

The *ortho*-iodonium ylide precursor **7b** was used to produce [^{18}F]**8** in preliminary PET imaging studies in one rhesus monkey. Metabolism of [^{18}F]**8** was extremely slow, with >90 % of intact radiotracer up to 90 min after injection. PET images and regional time-activity curves (TACs) of [^{18}F]**8** from the baseline and blocking scans are shown in Figure 3 and Figure 4. Baseline scan showed high uptake of the radiotracer, particularly in cortical regions (Figure 3, middle). Regional concentrations of the radiotracer reached peak levels within 20 min after injection, followed by a moderate rate of washout over time (Figure 4A). Pre-treatment of the animal with the 11β-HSD1 inhibitor ASP3662 (0.3 mg/kg) reduced activity uptake in all brain regions (Figure 3, bottom), indicating the binding specificity of the radiotracer *in vivo* (Figure 4B).

Regional TACs were processed with the one tissue compartment (1TC) model[34] to generate the regional volume of distribution (V_T, Table 3). In the blocking study, V_T was significantly reduced in all regions. Receptor occupancy was calculated to be 98% from the occupancy plot, with non-displaceable distribution volume (V_{ND}) of 3.5 mL/cm^{-3}. Regional BP_{ND} values calculated

from 1TC V_T in the baseline and V_{ND} from the blocking scan are shown in Table 3. The rank order of BP_{ND} in various regions are as follows: occipital cortex > cingulate cortex ≈ temporal cotex > pons > cerebellum > putamen > insula > brainstem > frontal cortex > caudate > thalamus. Levels of specific binding were high for [^{18}F]**8**, consisting of up to 77% of the signals in high binding regions.

CONCLUSIONS

The enzyme 11β-HSD1 is an important target for therapeutic development. We aimed to develop a PET imaging agent for 11β-HSD1 based on the potent and selective inhibitor AS2471907. Recently developed iodonium chemistry was explored to prepare two iodonium ylide precursors (**7a** and **7b**) for radiofluorination. Optimization of radiolabeling conditions indicated that DMF was the solvent of choice, and combination of TEAB/KOTf or TEAB alone gave the best radiochemical yield for ^{18}F-fluorination of precursors **7a** and **7b**, respectively, with the *ortho*-iodonium ylide precursor **7b** giving higher radiolabeling yield and molar activity in the synthesis of radiotracer [^{18}F]**8**. Preliminary PET imaging experiments in rhesus monkeys indicate that [^{18}F]**8** is a highly specific radiotracer with suitable properties for imaging 11β-HSD1 in the primate brain. Further evaluation of this novel radiotracer in non-human primates and humans is currently underway.

EXPERIMENTAL SECTION

Chemistry

General. All reagents and solvents were purchased from commercial sources (e.g., Sigma-Aldrich) and used without further purification unless noted otherwise. 2,6-Difluorophenol (**1a**) and

2,4-difluorophenol (**1b**) were obtained from FisherSci. Proton (^{1}H, 400 MHz or 600 MHz) and carbon (^{13}C, 151 MHz) nuclear magnetic resonance (NMR) spectra were recorded on an Agilent 400 MHz (A400a) or 600 MHz (A600a) spectrometer. Chemical shifts are reported in parts per million, with the solvent resonance as the internal standard (^{1}H NMR, $CDCl_3$: 7.26 ppm; DMSO-d_6: 2.49 ppm). Melting point was determined on an Electralthermo MelTemp instrument. High-resolution mass spectrometry (HRMS) was obtained on a Thermo LTQ Orbitrap spectrometer.

AS2471907 (**8**) and ASP3662 were provided by Astellas Pharma, and their synthesis has been reported previously.[19, 20, 35]

*Ethyl 2-(2,6-difluoro-4-iodophenoxy)-2-methylpropanoate (**2a**)*: To a solution of **1a** (6.8 g, 52.35 mmol), iodine (20.0 g, 78.80 mmol) and potassium iodide (13.0 g, 78.31 mmol) in de-ionized (DI) water (100 mL) was added dropwise a solution of sodium hydroxide (4.3 g, 105 mmol) in DI water (25 mL) at 0 ^{o}C. Then the reaction mixture was warmed to room temperature and kept stirring for 2 h. The reaction was neutralized with a solution of ammonium chloride in DI water followed by a solution of sodium thiosulfate in DI water until de-colorization. This mixture was then extracted with *t*-butyl methyl ether. The combined organic extracts were dried over $MgSO_4$ and concentrated *in vacuo*. To a solution of this crude product and ethyl 2-bromoisobutyrate (14.0 mL, 95.39 mmol) in DMF (100 mL) was added K_2CO_3 (22.0 g, 159.18 mmol) under argon. The reaction mixture was stirred at 80 ˚C for 3 h. After cooling to room temperature, the mixture was poured into ice cold H_2O (200 mL) and extracted with EtOAc (50 mL × 3). The combined organic phase was dried over $MgSO_4$ and concentrated *in vacuo*. The crude product was purified on a silica gel column, eluting with gradient 0 - 10% EtOAc/hexane to afford compound **2a** as a clear oil (10.0 g, 52%). ^{1}H NMR ($CDCl_3$, 400 MHz): δ 7.23 (d, J = 7.18 Hz, 2H), 4.23 (q, J = 7.14 Hz, 2H), 1.53 (s, 6H), 1.29 (t, J = 7.14 Hz, 3H).

*Ethyl 2-(2,4-difluoro-6-iodophenoxy)-2-methylpropanoate (**2b**)*: Compound **2b** was prepared in procedures similar to those described above for compound **2a**. Yield: 52%. ^{1}H NMR ($CDCl_3$, 400 MHz): δ 7.35-7.27 (m, 1H), 6.88-6.78 (m, 1H), 4.26 (q, J = 7.12 Hz, 2H), 1.53 (s, 6H), 1.29 (t, J = 7.12 Hz, 3H).

*2-(2,6-difluoro-4-iodophenoxy)-2-methylpropanoic acid (**3a**)*: To a solution of compound **2a** (6.0 g, 16.21 mmol) in EtOH (30 mL) was added dropwise a 3M solution of NaOH in DI water (11 mL, 33.00 mmol) at 0 °C and the mixture was stirred at room temperature for 3 h. The mixture was then poured into ice H_2O (50 mL) and washed with diisopropyl ether/heptane (v/v, 1/1, 20 mL × 2). The aqueous layer was separated, acidified with concentrated HCl to pH = 4, and then the cloudy solution was extracted with ethyl acetate (30 mL × 3). The combined organic phase was dried over $MgSO_4$, and concentrated *in vacuo* to afford compound **3a** as a light brown solid (4.75 g, 86%). The product was used in the next step without further purification. ^{1}H NMR ($CDCl_3$, 400 MHz): δ 7.30 (d, J = 6.83 Hz, 2H), 1.58 (s, 6H).

*2-(2,4-difluoro-6-iodophenoxy)-2-methylpropanoic acid (**3b**)*: Compound **3b** was prepared in procedures similar to those described above for compound **3a**. Yield: 86%. ^{1}H NMR ($CDCl_3$, 400 MHz): δ 7.34 (dt, J = 7.22, 2.17 Hz, 1H), 6.88 (td, J = 8.06, 2.92 Hz, 1H), 1.63 (s, 6H).

*2-chloro-N'-(2-(2,6-difluoro-4-iodophenoxy)-2-methylpropanoyl)benzohydrazide (**4a**)*: To a solution of compound **3a** (4.74 g, 13.87 mmol) in anhydrous CH_2Cl_2 (30 mL) under argon was added 1,1'-carbonyldiimidazole (CDI, 2.40 g, 14.36 mmol). The reaction mixture was stirred at room temperature for 1 h and 2-chlorobenzohydrazide (2.50 g, 14.36 mmol) was added. After stirring for 16 h, the reaction was quenched with DI water (50 mL) and extracted with CH_2Cl_2 (30 mL × 3). The combined organic phase was dried over $MgSO_4$, and concentrated *in vacuo*. The crude product was purified on a silica gel column, eluting with gradient 20 - 40% EtOAc/hexane

to afford compound **4a** as an off-white solid (3.88 g, 57%). ^{1}H NMR ($CDCl_3$, 400 MHz): δ 9.71 (d, J = 6.40 Hz, 1H), 9.15 (d, J = 6.49 Hz, 1H), 7.85 (d, J = 7.51 Hz, 1H), 7.44 (q, J = 7.82 Hz, 2H), 7.37 (t, J = 7.61 Hz, 1H), 7.32 (d, J = 6.81 Hz, 2H), 1.57 (s, 6H).

*2-chloro-N'-(2-(2,4-difluoro-6-iodophenoxy)-2-methylpropanoyl)benzohydrazide (**4b**):* Compound **4b** was prepared in procedures similar to those described above for compound **4a**. Yield: 57%. ^{1}H NMR ($CDCl_3$, 400 MHz): δ 9.63 (d, J = 6.42 Hz, 1H), 9.22-9.09 (m, 1H), 7.84 (d, J = 7.65 Hz, 1H), 7.42 (q, J = 7.76 Hz, 2H), 7.37 (t, J = 7.02 Hz, 2H), 6.90 (dt, J = 7.97, 2.94 Hz, 1H), 1.64 (s, 6H).

*2-(2-chlorophenyl)-5-(2-(2,6-difluoro-4-iodophenoxy)propan-2-yl)-1,3,4-oxadiazole (**5a**)*: To a solution of compound **4a** (3.88 g, 7.84 mmol) and 2-chloro-1,3-dimethylimidazolinium chloride (DMC, 2.20 g, 11.71 mmol) in anhydrous CH_2Cl_2 (70 mL) was slowly added triethylamine (TEA, 3.3 mL, 23.68 mmol) at 0 ^{o}C. After stirring at 0 ^{o}C for 1 h, the reaction was quenched with DI water (50 mL) and extracted with CH_2Cl_2 (25 mL × 2). The combined organic phase was dried over $MgSO_4$, and concentrated *in vacuo*. The crude product was purified on a silica gel column, eluting with gradient 0-20% EtOAc/hexane to afford compound **5a** as a colorless oil (2 g, 53%). ^{1}H NMR ($CDCl_3$, 400 MHz): δ 7.99 (d, J = 7.72 Hz, 1H), 7.55 (d, J = 7.98 Hz, 1H), 7.47 (t, J = 7.70 Hz, 1H), 7.41 (t, J = 7.51 Hz, 1H), 7.20 (d, J = 6.95 Hz, 1H overlap with m, 1H), 1.90 (s, 6H).

*2-(2-chlorophenyl)-5-(2-(2,4-difluoro-6-iodophenoxy)propan-2-yl)-1,3,4-oxadiazole (**5b**):* Compound **5b** was prepared in procedures similar to those described above for compound **5a**. Yield: 53%. ^{1}H NMR ($CDCl_3$, 400 MHz): δ 8.01 (d, J = 7.70 Hz, 1H), 7.56 (d, J = 8.03 Hz, 1H), 7.48 (t, J = 7.66 Hz, 1H), 7.41 (t, J = 7.53 Hz, 1H), 7.31 (d, J = 7.33 Hz, 1H), 6.79 (t, J = 10.05 Hz, 1H), 1.95 (s, 6H).

*3-(2-chlorophenyl)-5-(2-(2,6-difluoro-4-iodophenoxy)propan-2-yl)-4-methyl-4H-1,2,4-triazole (**6a**):* A mixture of compound **5a** (0.70 g, 1.47 mmol) and methylamine trifluoroacetate (3.20 g, 22.06 mmol, prepared by combining equal stoichiometry ratio of methylamine and trifluoroacetic acid in methanol followed by removal of solvent *in vacuo*) and molecular sieve powder (0.70 g) were suspended in methylamine (2M MeOH solution, 15.0 mL, 30.00 mmol). The reaction mixture was heated in a sealed tube at 150 ^{o}C for 48 h. After the reaction was cooled to room temperature, molecular sieves were removed via filtration and the filtrate was concentrated *in vacuo.* The crude compound was purified on a silica gel column, eluting with gradient 0-10% EtOH/EtOAc to afford compound **6a** as a light brown solid (0.2 g, 28%). ^{1}H NMR ($CDCl_3$, 400 MHz): δ 7.58-7.43 (m, 3H), 7.41 (t, J = 7.32 Hz, 1H), 7.23 (s, 2H overlap with $CHCl_3$ solvent peak), 3.75 (s, 3H), 1.87 (s, 6H).

*3-(2-chlorophenyl)-5-(2-(2,4-difluoro-6-iodophenoxy)propan-2-yl)-4-methyl-4H-1,2,4-triazole (**6b**):* Compound **6b** was prepared in procedures similar to those described above for compound **6a**. Yield: 28%. ^{1}H NMR ($CDCl_3$, 400 MHz): δ 7.56-7.42 (m, 3H), 7.44-7.34 (m, 1H), 7.36-7.26 (m, 1H), 6.85-6.73 (m, 1H), 3.74 (s, 3H), 1.91 (s, 6H).

*8-((4-((2-(5-(2-chlorophenyl)-4-methyl-4H-1,2,4-triazol-3-yl)propan-2-yl)oxy)-3,5-difluorophenyl)-λ^3-iodaneylidene)-6,10-dioxaspiro4.5decane-7,9-dione (**7a**)*: To a solution of compound **6a** (100 mg, 0.20 mmol) in $CHCl_3$ (3.0 mL) was added trifluoroacetic acid (0.48 mL, 6.23 mmol). Oxone (300 mg, 0.98 mmol) was added and the reaction mixture was stirred at room temperature for 2 h. Volatile contents were then removed *in vacuo*. The dried residue was suspended in EtOH (2 mL) and 6,10-dioxaspiro4.5decane-7,9-dione (**9**, 44 mg, 0.31 mmol) was added followed by 10% Na_2CO_3 (aq) until pH = 10. The reaction mixture was stirred for 3 h, diluted with water, and extracted with CH_2Cl_2 (3 mL × 3). The combined organic phase was dried

over $MgSO_4$ and concentrated *in vacuo*. The crude product was purified on a silica gel column, eluting with gradient 0-10% EtOH/EtOAc to afford compound **7a** as a white solid (78 mg, 58%). This compound can be further purified via trituration with a solvent mixture of EtOAc and hexane. M. P. 124 - 128 ^{o}C; ^{1}H NMR (600 MHz, DMSO-d_6): δ 7.72 (d, J = 7.85 Hz, 1H), 7.67-7.62 (m, 1H), 7.68-7.45 (m, 4H), 3.67 (s, 3H), 1.97-1.91 (m, 4H), 1.80 (s, 6H), 1.71-1.62 (m, 4H); ^{13}C NMR (151 MHz, DMSO-d_6): δ 164.32 (2C), 155.76, 155.21, 134.47, 132.58 (2C), 132.13 (2C), 129.95 (2C), 121.34 (2C), 126.51, 118.06, 117.87, 114.38, 81.94, 57.48, 37.42 (2C), 32.41, 26.09 (2C), 23.39 (2C). HRMS: calculated for $C_{26}H_{23}ClF_2IN_3O_5$ (M + H^+): 658.0418; found: 658.0412.

*8-((2-((2-(5-(2-chlorophenyl)-4-methyl-4H-1,2,4-triazol-3-yl)propan-2-yl)oxy)-3,5-difluorophenyl)-λ^3-iodaneylidene)-6,10-dioxaspiro4.5decane-7,9-dione (**7b**):* Compound **7b** was prepared in procedures similar to those described above for compound **7a**. Yield: 58%. M. P. 125 - 128 ^{o}C; ^{1}H NMR (600 MHz, ppm, DMSO-d_6): δ 7.68 (d, J = 7.94 Hz, 1H), 7.64-7.60 (m, 1H), 7.58-7.54 (m, 1H), 7.53-7.48 (m, 2H overlap), 7.48-7.46 (m, 1H), 3.60 (s, 3H), 1.92 (t, J = 7.30 Hz, 4H), 1.88 (s, 6H), 1.64 (t, J = 7.36 Hz, 4H); ^{13}C NMR (151 MHz, ppm, DMSO-*d6*): δ 163.89 (2C), 156.73, 154.20, 133.87 (2C overlap), 133.10 (2C overlap), 132.80, 130.21 (2C overlap), 128.12 (2C overlap), 127.10 (2C overlap), 112.77 (2C), 82.06, 59.81, 37.12 (2C), 32.37, 26.91 (2C), 23.15 (2C). HRMS: calculated for $C_{26}H_{23}ClF_2IN_3O_5$ (M + Na^+): 680.0231; found: 680.0276.

*6,10-dioxaspiro4.5decane-7,9-dione (**9**, SPI-5)*. Compound **9** was prepared in procedures described by Cai *et al.*[26] ^{1}H NMR ($CDCl_3$, 400 MHz): δ 3.62 (s, 2H), 2.26-2.15 (m, 4H), 1.96-1.80 (m, 4H).

Radiochemistry

[^{18}O]H_2O was obtained from Huayi Isotopes (Toronto, Canada). Anion exchange Chromafix cartridges (PS-HCO_3) were purchased from Macherey-Nagel (Dueringen, Germany). Solid-phase extraction (SPE) SepPak cartridges were purchased from Waters Associates (Milford, MA, USA). The HPLC system used for purification of crude product included a Shimadzu LC-20A pump, a Knauer K200 UV detector, and a Bioscan γ-flow detector, with a Prodigy C18 ODS(3) semi-preparative column (10 μm, 10 × 250 mm, Phenomenex, Torrance, CA). The HPLC system used for quality control tests was composed of a Shimadzu LC-20A pump, a Shimadzu SPD-M20A PDA or SPD-20A UV detector, a Bioscan γ-flow detector, with a Luna C18(2) column (5 μm, 4.6 × 250 mm, Phenomenex, Torrance, CA, USA).

Optimized radiosynthesis of 3-(2-chlorophenyl)-5-(2-(2,6-difluoro-4-(fluoro-^{18}F)phenoxy)propan-2-yl)-4-methyl-4H-1,2,4-triazole (p-[^{18}F]**8***).* ^{18}F-Fluoride was produced via the ^{18}O(p, n)^{18}F nuclear reaction in a 16.5-MeV GE PETtrace cyclotron (Uppsala, Sweden). The cyclotron produced ^{18}F-fluoride solution in [^{18}O]H_2O was transferred to a lead-shielded hot cell with a GE TRACERlab FXN Pro module for automated synthesis or with a collection vial for manual synthesis. The radioactivity was trapped on a Chromafix (PS-HCO_3, Macherey-Nagel, Dueringen, Germany) separation cartridge activated with 10 mL ethanol, followed by 10 mL 90 mg/mL KOTf solution in sterile H_2O, and finally 10 mL sterile H_2O. The ^{18}F-fluoride was eluted off the cartridge into a v-vial with a solution of TEAB (2 mg, 10.5 μmol, 1.8-3.5 equiv) and KOTf (5 mg, 26.5 μmol, 4.4-8.8 equiv) in 1 mL of MeCN/water (7:3, v/v). The solvent was removed under argon at 110 ºC, and dried azeotropically with the addition of 2 × 1 mL of MeCN. Precursor **7a** (2-2.5 mg, 3-6 μmol) in DMF (0.5 mL) was added to the reaction vessel, and the resulting solution was heated at 150 ºC for 10 min. After cooling, the crude product was pre-purified by solid phase extraction on a SepPak cartridge, eluted with 1 mL of EtOH, diluted with 3 mL of

hydrochloric acid (0.04 N), and then loaded onto a semi-preparative Prodigy C18 ODS(3) HPLC column for purification. The column was eluted with a mixture of 45% MeCN and 55% 0.04 N HCl (v/v) at a flow rate of 5 mL/min. The eluent was monitored by a UV detector and a radioactivity detector. The fraction containing *p*-[^{18}F]**8** was collected, diluted with 50 mL of DI water and passed through a Waters Classic C18 SepPak cartridge. The cartridge was rinsed with 10 mL of 0.001 N HCl and air dried. The radioactive product, trapped on the SepPak, was recovered by elution with 1 mL of absolute EtOH (USP), followed by 3 mL of USP saline into a 10 mL syringe barrel. The resulting EtOH-saline solution was then passed through a sterile membrane filter (0.22 μm) for terminal sterilization and collected in a sterile vial pre-charged with 7 mL of USP saline and 20 μL 8.4% USP $NaHCO_3$, affording a formulated I.V. solution ready for dispensing and injection.

*Optimized radiosynthesis of 3-(2-chlorophenyl)-5-(2-(2,4-difluoro-6-(fluoro-^{18}F)phenoxy)propan-2-yl)-4-methyl-4H-1,2,4-triazole (o-[^{18}F]**8**).* Radiosynthesis, formulation, and characterization were the same as for *p*-[^{18}F]**8**, except for the following: The Chromafix (PS-HCO_3) separation cartridge was activated with 10 mL ethanol followed by 10 mL sterile H_2O. The ^{18}F-fluoride was eluted off the cartridge into a v-vial with a solution of TEAB (2 mg, 10.5 μmol, 1.8-3.5 equiv) in 1 mL of MeCN/water (7:3, v/v).

*Quality Control and Analytical HPLC Conditions for [^{18}F]**8**.* Quality control of the chemical purity, radiochemical purity, and molar activity of [^{18}F]**8** was determined by analytical HPLC analysis of the final product solution. The identity of [^{18}F]**8** was confirmed by co-injection of the product with the unlabeled standard (**8**) and detection of a single UV peak at 230 nm on the chromatogram. Chemical and radiochemical purity > 99% by analytical HPLC eluting with a

mobile phase of 52% MeCN and 48% 0.1 M ammonium formate solution (pH 4.2) with 0.5% acetic acid at aflow rate of 2.0 mL/min.

PET Procedures.

Imaging in Nonhuman Primates. Experiments were performed in rhesus monkeys (*Macaca mulatta*) according to a protocol approved by the Yale University Institutional Animal Care and Use Committee. The animals were fasted overnight prior to imaging. The animals were immobilized with ketamine (10 mg/kg intramuscularly) and anesthetized with 1-2% isoflurane. An indwelling port was surgically placed in a femoral artery for arterial blood sampling for metabolite analysis.[36] A water-jacket heating pad was used to maintain body temperature. The animal was attached to a physiological monitor, and vital signs (pulse rate, blood pressure, respirations, EKG, ETCO2, and body temperature) were continuously monitored. Baseline and blocking scans were performed on a Siemens FOCUS 220 camera. Before radiotracer injection, a 9-minute transmission scan was obtained for attenuation correction. ^{18}F-**8** was injected intravenously over 3 min as a bolus (~185 MBq/10 mL). PET scans were acquired over 2 h. In the blocking scan the 11β-HSD1 inhibitor ASP3662 (0.3 mg/kg) was administered over 5 min starting at 15 min before radiotracer injection.

Image Reconstruction and Analysis. Procedures for PET image reconstruction and definition of regions of interest (ROIs) have been described previously.[36] Emission data were attenuation corrected using the transmission scan, and dynamic images (33 frames over 120 min) were reconstructed using a filtered back-projected algorithm with a Shepp-Logan filter. ROIs were defined from a single representative anatomic rhesus MR image registered to a template image.

For each PET scan, radiotracer concentrations over time were measured in the ROIs to generate the regional time-activity curves (TACs).

Regional TACs were analyzed to calculate regional volume of distribution (V_T, mL/cm^{-3}) using the one-tissue compartmental model (1TC) [34]. Target occupancy by the blocking drug was obtained from occupancy plot using the regional V_T from the baseline scan and V_T difference between baseline and blocking scans according to the method of Cunningham *et al.* [37].

Regional non-displaceable binding potential (BP_{ND}) was calculated using the 1TC V_T values from the baseline scan and the non-displaceable distribution volume (V_{ND}) derived from the occupancy plot to assess levels of specific binding, with $BP_{ND} = (V_{T\ ROI} - V_{ND})/V_{ND}$.

AUTHOR INFORMATION

Corresponding Author: *E-mail: songye.li@yale.edu Telephone: 203-785-3605 Fax: 203-785-3107 and jason.cai@yale.edu, Telephone: 203-785-7691.

Author Contributions: E.B. and W.Z. contributed equally to this work. All authors contributed to and approved the final version of this manuscript.

ACKNOWLEDGEMENT

The authors thank the staff at the Yale PET Center for their expert technical assistance.

ABBREVIATIONS USED

11β-HSD1, 11-beta hydroxysteroid dehydrogenase type 1; PET, positron emission tomography; CDI, 1,1′-Carbonyldiimidazole; DMC, 2-chloro-1,3-dimethylimidazolinium chloride; MeCN, acetonitrile; KOTf, potassium trifluoromethanesulfonate; TBAOTf, tetrabutylammonium trifluoromethanesulfonate; K_2CO_3, potassium carbonate; $CsCO_3$, cesium carbonate; TEAB, tetraethylammonium bicarbonate; K222, Kryptofix® 222; RCC, radiochemical conversion; RCY, radiochemical yield; MA EOS, molar activity at end of synthesis.

REFERENCES

1. Wyrwoll, C. S., Holmes, M. C., and Seckl, J. R. (2011) 11β-hydroxysteroid dehydrogenases and the brain: from zero to hero, a decade of progress, *Front Neuroendocrinol 32*, 265-286.

2. Leckie, C. M., Welberg, L. A., and Seckl, J. R. (1998) 11β-hydroxysteroid dehydrogenase is a predominant reductase in intact rat Leydig cells, *J Endocrinol 159*, 233-238.

3. Anderson, A., and Walker, B. R. (2013) 11β-HSD1 inhibitors for the treatment of type 2 diabetes and cardiovascular disease, *Drugs 73*, 1385-1393.

4. Paterson, J. M., Morton, N. M., Fievet, C., Kenyon, C. J., Holmes, M. C., Staels, B., Seckl, J. R., and Mullins, J. J. (2004) Metabolic syndrome without obesity: hepatic overexpression of 11β-hydroxysteroid dehydrogenase type 1 in transgenic mice, *Proc Natl Acad Sci USA 101*, 7088-7093.

5. Masuzaki, H., Yamamoto, H., Kenyon, C. J., Elmquist, J. K., Morton, N. M., Paterson, J. M., Shinyama, H., Sharp, M. G., Fleming, S., Mullins, J. J., Seckl, J. R., and Flier, J. S. (2003) Transgenic amplification of glucocorticoid action in adipose tissue causes high blood pressure in mice, *J Clin Invest 112*, 83-90.

6. Masuzaki, H., Paterson, J., Shinyama, H., Morton, N. M., Mullins, J. J., Seckl, J. R., and Flier, J. S. (2001) A transgenic model of visceral obesity and the metabolic syndrome, *Science 294*, 2166-2170.

7. Stimson, R. H., Andrew, R., McAvoy, N. C., Tripathi, D., Hayes, P. C., and Walker, B. R. (2011) Increased whole-body and sustained liver cortisol regeneration by 11β-hydroxysteroid dehydrogenase type 1 in obese men with type 2 diabetes provides a target for enzyme inhibition, *Diabetes 60*, 720-725.

8. Yau, J. L., Noble, J., Kenyon, C. J., Hibberd, C., Kotelevtsev, Y., Mullins, J. J., and Seckl, J. R. (2001) Lack of tissue glucocorticoid reactivation in 11β-hydroxysteroid dehydrogenase type 1 knockout mice ameliorates age-related learning impairments, *Proc Natl Acad Sci USA 98*, 4716-4721.

9. Sooy, K., Webster, S. P., Noble, J., Binnie, M., Walker, B. R., Seckl, J. R., and Yau, J. L. (2010) Partial deficiency or short-term inhibition of 11β-hydroxysteroid dehydrogenase type 1 improves cognitive function in aging mice, *J Neurosci 30*, 13867-13872.

10. Sooy, K., Noble, J., McBride, A., Binnie, M., Yau, J. L., Seckl, J. R., Walker, B. R., and Webster, S. P. (2015) Cognitive and disease-modifying effects of 11β-hydroxysteroid dehydrogenase type 1 inhibition in male Tg2576 mice, a model of Alzheimer's disease, *Endocrinology 156*, 4592-4603.

11. Sandeep, T. C., Yau, J. L., MacLullich, A. M., Noble, J., Deary, I. J., Walker, B. R., and Seckl, J. R. (2004) 11β-hydroxysteroid dehydrogenase inhibition improves cognitive function in healthy elderly men and type 2 diabetics, *Proc Natl Acad Sci USA 101*, 6734-6739.

12. Sorensen, B., Rohde, J., Wang, J., Fung, S., Monzon, K., Chiou, W., Pan, L., Deng, X., Stolarik, D., Frevert, E. U., Jacobson, P., and Link, J. T. (2006) Adamantane 11β-HSD1 inhibitors: application of an isocyanide multicomponent reaction, *Bioorg Med Chem Lett 16*, 5958-5962.

13. Marek, G. J., Katz, D. A., Meier, A., Greco, N. t., Zhang, W., Liu, W., and Lenz, R. A. (2014) Efficacy and safety evaluation of HSD-1 inhibitor ABT-384 in Alzheimer's disease, *Alzheimers Dement 10*, S364-373.

14. Webster, S. P., McBride, A., Binnie, M., Sooy, K., Seckl, J. R., Andrew, R., Pallin, T. D., Hunt, H. J., Perrior, T. R., Ruffles, V. S., Ketelbey, J. W., Boyd, A., and Walker, B. R. (2017)

Selection and early clinical evaluation of the brain-penetrant 11β-hydroxysteroid dehydrogenase type 1 (11β-HSD1) inhibitor UE2343 (Xanamem), *Br J Pharmacol 174*, 396-408.

15. Siu, M., Johnson, T. O., Wang, Y., Nair, S. K., Taylor, W. D., Cripps, S. J., Matthews, J. J., Edwards, M. P., Pauly, T. A., Ermolieff, J., Castro, A., Hosea, N. A., LaPaglia, A., Fanjul, A. N., and Vogel, J. E. (2009) N-(Pyridin-2-yl) arylsulfonamide inhibitors of 11β-hydroxysteroid dehydrogenase type 1: Discovery of PF-915275, *Bioorg Med Chem Lett 19*, 3493-3497.

16. Zhu, Y., Olson, S. H., Graham, D., Patel, G., Hermanowski-Vosatka, A., Mundt, S., Shah, K., Springer, M., Thieringer, R., Wright, S., Xiao, J., Zokian, H., Dragovic, J., and Balkovec, J. M. (2008) Phenylcyclobutyl triazoles as selective inhibitors of 11β-hydroxysteroid dehydrogenase type 1, *Bioorg Med Chem Lett 18*, 3412-3416.

17. Robl, J. A. W., H.; Li, J. J.; Hamann, L.; Simpkins, L.; Golla, R.; Li, Y.-X.; Seethala, R.; Zvyaga, T.; Harper, T.; Hsueh, M.; Wang, M.; Hansen, L.; Patel, C.; Azzara, A.; Rooney, S.; Sheriff, S.; Morin, P.; Camac, D.; Harrity, T.; Zebo, R.; Ponticiello, R.; Morgan, N.; Taylor, J.; Gordon, D. (2012) Optimization of triazolopyridine based 11β-hydroxysteroid dehydrogenase type-1 (11β-HSD1) inhibitors leading to the discovery of the clinical candidate BMS-770767, *Abstracts of Papers, 244th ACS National Meeting & Exposition, Philadelphia, United States*.

18. Kiso, T., Sekizawa, T., Uchino, H., Tsukamoto, M., and Kakimoto, S. (2018) Analgesic effects of ASP3662, a novel 11β-hydroxysteroid dehydrogenase 1 inhibitor, in rat models of neuropathic and dysfunctional pain, *Br J Pharmacol 175*, 3784-3796.

19. Yoshimura, S., Kawano, N., Kawano, T., Sasuga, D., Koike, T., Watanabe, H., Fukudome, H., Shiraishi, N., Munakata, R., and Hoshii, H. (2013) Triazole derivative or salt thereof. U.S. Patent Application Publication. No. 8,377,923.

20. Iwashita, A., Fushiki, H., Fujita, Y., Murakami, Y., and Noda, A. (2016) Discovery of a novel radioligand [^{11}C] AS2471907 for PET imaging of the brain 11β-HSD1, *J Nucl Med 57*, 1050.

21. Huang, Y., Planet, B., Nabulsi, N., Henry, S., Zheng, M.-Q., Lin, S.-F., Matuskey, D., Walzer, M., Marek, G., and Carson, R. (2016) First-in-human study of the 11β-hydroxysteroid dehydrogenase type 1 PET tracer [^{11}C]AS2471907, *J Nucl Med 57*, 580.

22. Brooks, A. F., Topczewski, J. J., Ichiishi, N., Sanford, M. S., and Scott, P. J. (2014) Late-stage [^{18}F]fluorination: new solutions to old problems, *Chem Sci 5*, 4545-4553.

23. Campbell, M. G., and Ritter, T. (2014) Late-stage fluorination: from fundamentals to application, *Org Process Res Dev 18*, 474-480.

24. Rotstein, B. H., Stephenson, N. A., Vasdev, N., and Liang, S. H. (2014) Spirocyclic hypervalent iodine(III)-mediated radiofluorination of non-activated and hindered aromatics, *Nat Commun 5*, 4365.

25. Rotstein, B. H., Wang, L., Liu, R. Y., Patteson, J., Kwan, E. E., Vasdev, N., and Liang, S. H. (2016) Mechanistic studies and radiofluorination of structurally diverse pharmaceuticals with spirocyclic iodonium(III) ylides, *Chem Sci 7*, 4407-4417.

26. Cai, Z., Li, S., Pracitto, R., Navarro, A., Shirali, A., Ropchan, J., and Huang, Y. (2017) Fluorine-18-Labeled Antagonist for PET Imaging of Kappa Opioid Receptors, *ACS Chem Neurosci 8*, 12-16.

27. Cardinale, J., Ermert, J., Humpert, S., and Coenen, H. H. (2014) Iodonium ylides for one-step, no-carrier-added radiofluorination of electron rich arenes, exemplified with 4-(([^{18}F]fluorophenoxy)-phenylmethyl)piperidine NET and SERT ligands, *RSC Advances 4*, 17293-17299.

28. Stephenson, N. A., Holland, J. P., Kassenbrock, A., Yokell, D. L., Livni, E., Liang, S. H., and Vasdev, N. (2015) Iodonium ylide-mediated radiofluorination of [^{18}F]FPEB and validation for human use, *J Nucl Med 56*, 489-492.

29. Mossine, A. V., Brooks, A. F., Makaravage, K. J., Miller, J. M., Ichiishi, N., Sanford, M. S., and Scott, P. J. (2015) Synthesis of [^{18}F]arenes via the copper-mediated [^{18}F]fluorination of boronic acids, *Org Lett 17*, 5780-5783.

30. Carroll, M. A., Nairne, J., Smith, G., and Widdowson, D. A. (2007) Radical scavengers: a practical solution to the reproducibility issue in the fluoridation of diaryliodonium salts, *J Fluorine Chem 128*, 127-132.

31. Ross, T. L., Ermert, J., Hocke, C., and Coenen, H. H. (2007) Nucleophilic ^{18}F-fluorination of heteroaromatic iodonium salts with no-carrier-added ^{18}F-fluoride, *J Am Chem Soc 129*, 8018-8025.

32. Zlatopolskiy, B. D., Zischler, J., Urusova, E. A., Endepols, H., Kordys, E., Frauendorf, H., Mottaghy, F. M., and Neumaier, B. (2015) A practical one-pot synthesis of positron emission tomography (PET) tracers via nickel-mediated radiofluorination, *ChemistryOpen 4*, 457-462.

33. Chun, J. H., Lu, S., Lee, Y. S., and Pike, V. W. (2010) Fast and high-yield microreactor syntheses of ortho-substituted [^{18}F]fluoroarenes from reactions of ^{18}F-fluoride ion with diaryliodonium salts, *J Org Chem 75*, 3332-3338.

34. Gunn, R. N., Gunn, S. R., and Cunningham, V. J. (2001) Positron emission tomography compartmental models, *J Cereb Blood Flow Metab 21*, 635-652.

35. Kiso, T., and Tsukamoto, M. (2013) Therapeutic agent for pain. U.S. Patent Application Publication No. 2013/0165491.

36. Li, S., Cai, Z., Zheng, M. Q., Holden, D., Naganawa, M., Lin, S. F., Ropchan, J., Labaree, D., Kapinos, M., Lara-Jaime, T., Navarro, A., and Huang, Y. (2018) Novel ^{18}F-Labeled kappa-Opioid Receptor Antagonist as PET Radiotracer: Synthesis and In Vivo Evaluation of ^{18}F-LY2459989 in Nonhuman Primates, *J Nucl Med 59*, 140-146.

37. Cunningham, V. J., Rabiner, E. A., Slifstein, M., Laruelle, M., and Gunn, R. N. (2010) Measuring drug occupancy in the absence of a reference region: the Lassen plot re-visited, *J Cereb Blood Flow Metab 30*, 46-50.

TABLES AND FIGURES

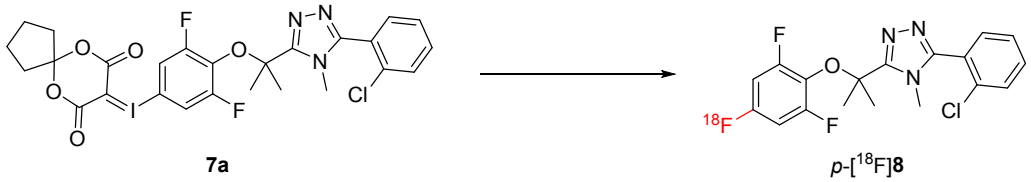

Table 1. Optimization on radiolabeling of precursor 7a

Entry	Base	Temp. (°C)	Time (min)	Solvent	RCC[a] (%)
1[b]	KOTf (170 µg), K_2CO_3 (1.7 µg)	120	10	MeCN	No reaction
2[b]	KOTf (170 µg), K_2CO_3 (1.7 µg)	120, 160, 200	10	DMSO	No reaction
3[b]	KOTf (170 µg), K_2CO_3 (1.7 µg)	120, 160, 200	10	DMF	2, 4.8, 8
4[b]	KOTf (0.5 mg), K_2CO_3 (5 µg)	120, 160, 200	10	DMF	3.4, 3.8, 6.7
5	KOTf (5 mg), K_2CO_3 (50 µg)	160	10	DMF	1.9
6	KOTf (5 mg), K_2CO_3 (50 µg), K222 (0.5 mg)	120, 160	10	DMF	0.5, 0.8
7	KOTf (5 mg), K_2CO_3 (50 µg), 18-Crown-6 (0.35 mg)	120, 160	10	DMF	0.8, 0.8
8	KOTf (5 mg), TEAB (0.25 mg)	120, 160	10	DMF	0.9, 1.7
9	KOTf (5 mg), TEAB (0.5 mg)	160	10	DMF	6.9
10	KOTf (5 mg), TEAB (1 mg)	160	10	DMF	6.7
11	KOTf (5 mg), TEAB (1.5 mg)	160	10	DMF	9.9
12	KOTf (5 mg), TEAB (2 mg)	160	10	DMF	12.4
13	TEAB (2 mg)	160	10	DMF	6.5

[a]Radiochemical conversion (RCC) is calculated as integration of the product peak on analytical HPLC.
[b]Elution of ^{18}F-fluoride with KOTf (5 mg) and K_2CO_3 (50 µg) followed by aliquoting to achieve the stated amount of reagents

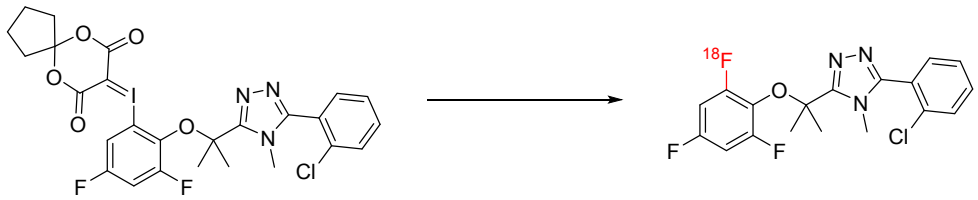

7b *o*-[^{18}F]**8**

Table 2. Base effect on radiolabeling of precursor 7b in DMF

Entry	Base	Temp. (°C)	Time (min)	RCC[a] (%)
1	KOTf (5 mg), TEAB (2 mg)	150	20	22
2	TBAOTf (5 mg), Cs_2CO_3 (5 µg)	160	20	2.5
3	TBAOTf (5 mg)	160	20	2.3
4	TEAB (2 mg)	150	10	34
5	TEAB (4 mg)	150	10	16
6	TEAB (8 mg)	150	10	28
7	TEAB (16 mg)	150	10	16

[a] Radiochemical conversion (RCC) was calculated as integration of the product peak on analytical HPLC.

Table 3. Regional distribution volume (V_T, mL/cm^3) and non-displaceable binding potentials (BP_{ND}) of baseline and blocking scans in the same monkey

ROI	V_T (mL/cm^3)		BP_{ND}	
	Baseline	**Blocking**	**Baseline**	**Blocking**
Caudate	5.5	3.4	0.55	-0.03
Cerebellum	9.5	3.6	1.71	0.03
Cingulate cortex	11.9	3.5	2.38	0.00
Frontal cortex	6.4	3.1	0.81	-0.11
Insula	7.8	3.3	1.22	-0.07
Occipital cortex	14.9	3.5	3.23	0.00
Pons	10.2	4.5	1.88	0.29
Putamen	9.4	3.9	1.67	0.11
Temporal cortex	11.8	3.3	2.35	-0.07
Thalamus	4.8	3.6	0.38	0.03

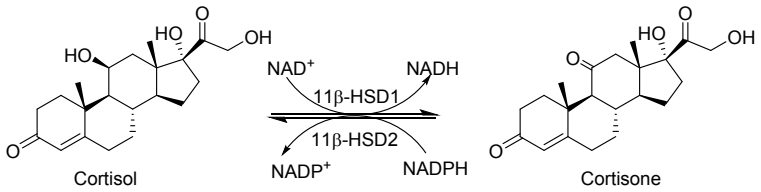

Figure 1. Inter-conversion of cortisone and cortisol via 11β-HSD isozymes

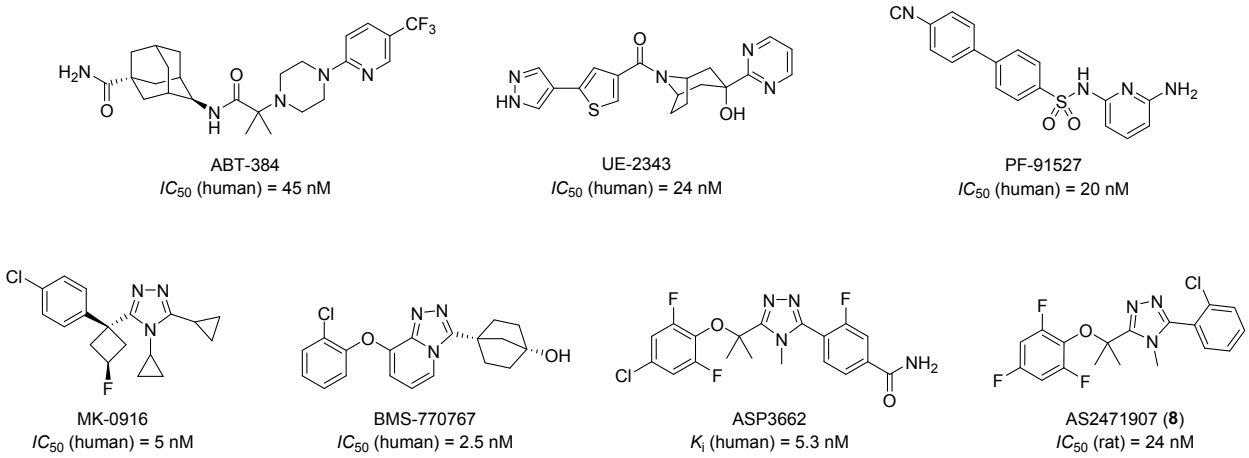

Figure 2. Inhibitors of 11β-HSD1 as drug candidates with half maximal inhibitory concentration (IC_{50}) and binding affinity (K_i)from the literatures. Compound **8**, the target molecule (the reference compound for radiolabeling in this study, included for structural comparison).

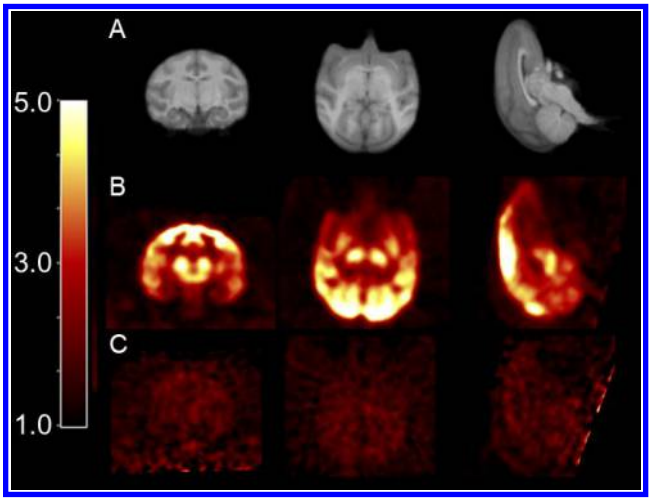

Figure 3. Template MRI (A), representative summed standardized uptake value (SUV) PET images (30 to 45 min post-injection) from a [^{18}F]**8** baseline scan (B) and a pre-blocking scan with 11β-HSD1 inhibitor ASP3662 (0.3 mg/kg) (C).

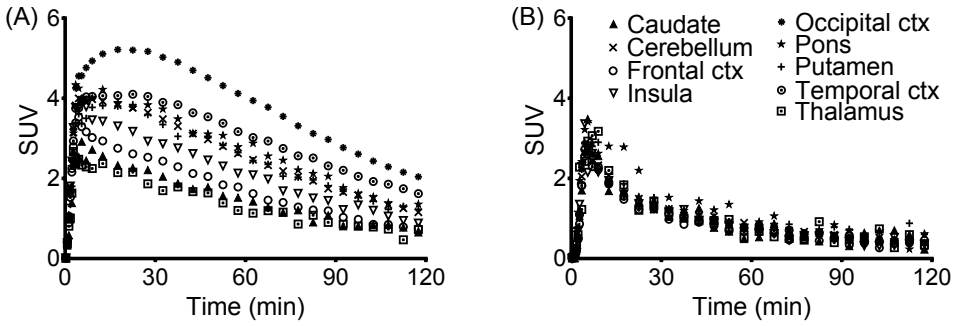

Figure 4. Regional time-activity curves from baseline (A) and blocking (B, 0.3 mg/kg of ASP3662) scans with [^{18}F]AS2471907.

Scheme 1. Radiosynthesis of [^{11}C]AS2471907.

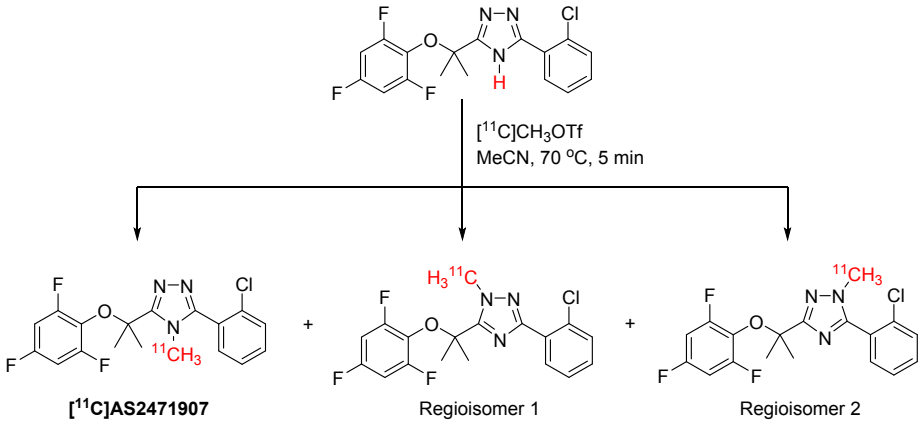

Scheme 2. Synthesis of *para*- and *ortho*-iodonium ylide precursors for radiofluorination.

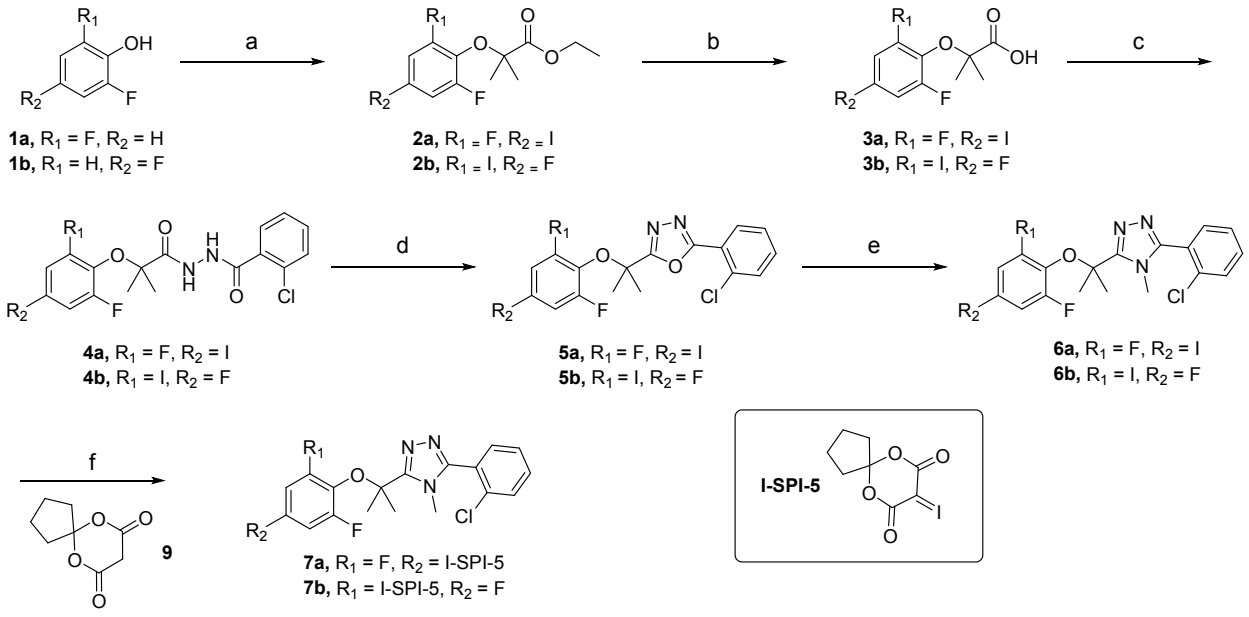

Reagents and conditions: (a) (1) I_2, NaOH, KI, H_2O, 0 °C, then r. t., 2 h; (2) Ethyl 2-bromoisobutyrate, K_2CO_3, DMF, 80 °C, 3 h. (b) (1) NaOH (aq.), EtOH, r. t., 2.5 h; (2) HCl, pH = 4. (c) 2-chlorobenzohydrazide, CDI, CH_2Cl_2, r.t., 16 h. (d) DMC, Et_3N, CH_2Cl_2, r. t., 1 h. (e) $MeNH_2$-TFA, $MeNH_2$/MeOH, 150 °C, 48 h. (f) (1) Oxone, TFA, $CHCl_3$, r.t., 2 h; (2) **9**, Na_2CO_3, EtOH, r.t., 3 h.